

Bulk matter evolution and extraction of jet transport parameter in heavy-ion collisions at RHIC

Xiao-Fang Chen,^{1,2} Carsten Greiner,² Enke Wang,¹ Xin-Nian Wang,^{3,2} and Zhe Xu^{4,2}

¹*Institute of Particle Physics and Key Laboratory of Quark & Lepton Physics, Huazhong Normal University, Wuhan 430079, China*

²*Institut für Theoretische Physik, Johann Wolfgang Goethe-Universität, Max-von-Laue-Str. 1, D-60438 Frankfurt am Main, Germany*

³*Nuclear Science Division, MS 70R0319, Lawrence Berkeley National Laboratory, Berkeley, CA 94720*

⁴*Frankfurt Institute for Advanced Studies, Ruth-Moufang-Str. 1, D-60438 Frankfurt am Main, Germany*

(Dated: November 2, 2018)

Within the picture of jet quenching induced by multiple parton scattering and gluon bremsstrahlung, medium modification of parton fragmentation functions and therefore the suppression of large transverse momentum hadron spectra are controlled by both the value and the space-time profile of the jet transport parameter along the jet propagation path. Experimental data on single hadron suppression in high-energy heavy-ion collisions at the RHIC energy are analyzed within the higher-twist (HT) approach to the medium modified fragmentation functions and the next-to-leading order (NLO) perturbative QCD (pQCD) parton model. Assuming that the jet transport parameter \hat{q} is proportional to the particle number density in both QGP and hadronic phase, experimental data on jet quenching in deeply inelastic scattering (DIS) off nuclear targets can provide guidance on \hat{q}_h in the hot hadronic matter. One can then study the dependence of extracted initial value of jet quenching parameter \hat{q}_0 at initial time τ_0 on the bulk medium evolution. Effects of transverse expansion, radial flow, phase transition and non-equilibrium evolution are examined. The extracted values are found to vary from $\hat{q}_0\tau_0 = 0.54 \text{ GeV}^2$ in the (1+3)d ideal hydrodynamic model to 0.96 GeV^2 in a cascade model, with the main differences coming from the initial non-equilibrium evolution and the later hadronic evolution. The overall contribution to jet quenching from the hadronic phase, about 22-44%, is found to be significant. Therefore, realistic description of the early non-equilibrium parton evolution and later hadronic interaction will be critical for accurate extraction of the jet transport parameter in the strongly interacting QGP phase in high-energy heavy-ion collisions.

PACS numbers: 12.38.Mh, 24.85.+p, 25.75.-q

I. INTRODUCTION

A large amount of experimental data from the Relativistic Heavy Ion Collider (RHIC) [1–4] strongly suggest that a novel form of matter, a strongly coupled quark gluon plasma (sQGP), may have been formed in the central region of high-energy heavy-ion collisions. Among the experimental evidences for the formation of sQGP are the jet quenching phenomena that include the strong suppression of hadron spectra with large transverse momentum in central $Au + Au$ collisions as compared to $p + p$ collisions [5, 6] and the disappearance of back-to-back correlations of large transverse momentum hadrons [7]. These jet quenching patterns observed at RHIC are in good agreement with the theoretical predictions for jet quenching [8–13] or suppression of large transverse momentum hadrons as a consequence of parton energy loss and medium modified parton fragmentation functions induced by multiple scattering as partons propagate through the dense medium after their initial production. The parton energy loss and medium modification of the fragmentation functions due to multiple parton scattering and induced gluon bremsstrahlung are

controlled by the jet transport parameter [14],

$$\hat{q}_R = \rho \int dq_T^2 \frac{d\sigma_R}{dq_T^2} q_T^2. \quad (1)$$

or the average squared transverse momentum broadening per unit length for a jet in color representation R , which is also related to the gluon distribution density of the medium [14, 15] and therefore characterizes the medium property as probed by an energetic jet. Here we consider a picture in which the jet parton interacts with medium particles or quasi-particles with cross section σ_R and ρ is the local particle density of the medium. Study of the jet quenching phenomena therefore can provide important information on the space-time profile of the jet transport parameter and consequently properties of the sQGP in heavy-ion collisions.

Extensive phenomenological studies on the suppression of single hadron spectra [13, 16–19] and dihadron correlations [20, 21] at large transverse momentum have been carried out since the first observation of the strong jet quenching phenomena. Recent emphasis of the phenomenological studies has been shifted to systematic analyses of the experimental data with different jet quenching models and qualitative extraction of the jet transport parameter [22–26]. In this paper, we will carry out phenomenological analysis of the suppression of sin-

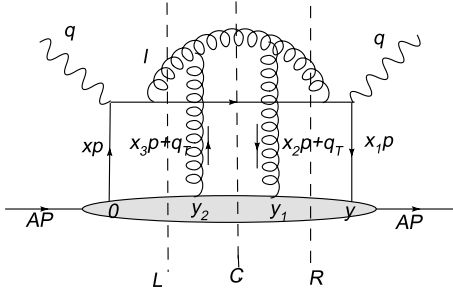


FIG. 1: A typical Feynman diagram for quark-gluon rescattering processes in DIS with three possible cuts, central(C), left(L), and right(R).

gle hadron spectra within the higher-twist (HT) formalism for medium modification of the parton fragmentation functions and the next-to-leading order perturbative QCD parton model [20] for initial jet production. We will calculate the single hadron suppression within three different models for the dynamical evolution of the bulk matter: (1+1)d Bjorken model, (1+3)d ideal hydrodynamic model and a parton cascade model. We will study in particular the effect of collective expansion, transverse flow, non-equilibrium and most importantly jet quenching in the hadronic phase of the bulk matter. Since the jet transport parameter is related to the gluon distribution density of the bulk medium, one expects it to be different in a QGP and hadronic matter. We will use the information on jet transport parameter in cold nuclei extracted from phenomenological studies of deeply inelastic scattering (DIS) off large nuclei [27] and extrapolate to a hot hadronic gas assuming that the gluon distribution in a nucleon in cold nuclei is the same as in a hot hadronic gas. This allows us to focus on the values of the jet transport parameter in a QGP that can be accommodated by the experimental data on single hadron suppression and the effect of dynamic evolution of the bulk medium.

The rest of the paper is organized as follows. In the next section, we will review the energy loss and modified fragmentation functions in hot nuclear medium within the HT approach and their dependence on the space-time profile of the jet transport parameter \hat{q}_R . We then describe the next-to-leading order (NLO) pQCD parton model for single hadron production in heavy-ion collisions in Sec. III. In Sec. IV, we will introduce three different dynamic evolutions for the bulk medium. The numerical calculations and phenomenological studies of the experimental data on single hadron suppression and extraction of the jet transport parameters within each dynamic model are carried out in Sec. V. Finally, we conclude in Sec. VI with a summary.

II. ENERGY LOSS AND MODIFIED FRAGMENTATION FUNCTIONS

Within the generalized factorization of twist-four processes, one can calculate the nuclear modification of fragmentation functions and the energy loss of a quark propagating through nuclear matter after it is produced via a hard process in DIS off a nuclear target [28, 29]. Within such HT approach, the medium modification to the quark fragmentation functions in DIS off a nuclear target is caused by multiple scattering between the struck quark and the nuclear medium on the quark's propagation path and the induced gluon bremsstrahlung as illustrated in Fig. (1). The medium modified quark fragmentation function,

$$\begin{aligned} \tilde{D}_q^h(z_h, Q^2) &= D_q^h(z_h, Q^2) + \frac{\alpha_s(Q^2)}{2\pi} \int_0^{Q^2} \frac{d\ell_T^2}{\ell_T^2} \\ &\times \int_{z_h}^1 \frac{dz}{z} \left[\Delta\gamma_{q \rightarrow qg}(z, x, x_L, \ell_T^2) D_q^h\left(\frac{z_h}{z}\right) \right. \\ &\quad \left. + \Delta\gamma_{q \rightarrow gq}(z, x, x_L, \ell_T^2) D_g^h\left(\frac{z_h}{z}\right) \right], \quad (2) \end{aligned}$$

takes a form very similar to the vacuum bremsstrahlung corrections that leads to the Dokshitzer-Gribov-Lipatov-Altarelli-Parisi (DGLAP) [30] evolution equations in pQCD for fragmentation functions, except that the medium modified splitting functions,

$$\begin{aligned} \Delta\gamma_{q \rightarrow qg}(z, x, x_L, \ell_T^2) &= \left[\frac{1+z^2}{(1-z)_+} T_{qg}^A(x, x_L) \right. \\ &\quad \left. + \delta(1-z) \Delta T_{qg}^A(x, x_L) \right] \frac{2\pi\alpha_s C_A}{\ell_T^2 N_c f_q^A(x)}; \quad (3) \end{aligned}$$

$$\Delta\gamma_{q \rightarrow gq}(z, x, x_L, \ell_T^2) = \Delta\gamma_{q \rightarrow qg}(1-z, x, x_L, \ell_T^2), \quad (4)$$

depend on the properties of the medium through the twist-four quark-gluon correlations inside the nucleus,

$$\begin{aligned} T_{qg}^A(x, x_L) &= \int \frac{d^2 q_T}{(2\pi)^2} \int \frac{dy^-}{2\pi} d\xi^- dy_2^- d^2 \xi_T e^{i(x+x_L)p^+ y^-} \\ &\times e^{ix_T p^+ \xi^- - i\bar{q}_T \bar{\xi}_T} \left\{ (1 - e^{-ix_L p^+ y_2^-}) (1 - e^{-ix_L p^+ (y^- - y_1^-)}) \right. \\ &\quad \left. + \frac{1-z}{2} \left[e^{-ix_L p^+ y_2^-} (1 - e^{-ix_L p^+ (y^- - y_1^-)}) \right. \right. \\ &\quad \left. \left. + e^{-ix_L p^+ (y^- - y_1^-)} (1 - e^{ix_L p^+ y_2^-}) \right] \right\} \theta(-y_2^-) \theta(y^- - y_1^-) \\ &\times \langle A | \bar{\psi}_q(0) \frac{\gamma^+}{2} F_{\sigma^+}(y_2^-) F^{+\sigma}(y_1^-, \xi_T) \psi_q(y^-) | A \rangle, \quad (5) \end{aligned}$$

where $\xi = y_1 - y_2$, y , y_1 and y_2 are space-time coordinates associated with the quark and gluon fields as illustrated in Fig. 1. Here we include contributions beyond the helicity approximation [29] and consider only the twist-four matrices that are enhanced by the large nuclear size. The relative transverse coordinate ξ_T is the Fourier conjugate of the transverse momentum q_T in the gluon distribution function. The momentum fraction

$$x_L = \frac{\ell_T^2}{2z(1-z)p^+ q^-}, \quad (6)$$

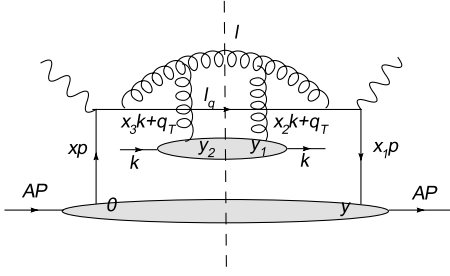


FIG. 2: Feynman diagram for induced gluon radiation in hot QGP medium that contributes the quark energy loss.

is the total (+component) longitudinal momentum transfer from the target to the propagating quark and radiated gluon with longitudinal momentum zq^- and transverse momentum ℓ_T . We impose kinematic constraints $x_L \leq 1$ and $\ell_T \leq \min[zE, (1-z)E]$ in the integration in Eq. (2). A similar (+) longitudinal momentum transfer

$$x_T = \frac{q_T^2 - 2q_T \cdot \ell_T}{2zp^+q^-}, \quad (7)$$

is also provided by the initial gluon with transverse momentum q_T . In the modified splitting function,

$$f_q^A(x) = \int \frac{dy^-}{2\pi} e^{ixp^+y^-} \langle A | \bar{\psi}_q(0) \frac{\gamma^+}{2} \psi_q(y^-) | A \rangle \quad (8)$$

is the quark distribution function which represents the production rate of the initial quark carrying $x = Q^2/2p^+q^-$ (the Bjorken variable) fraction of the nucleon (+) longitudinal momentum in DIS. The quark-gluon matrix element,

$$\Delta T_{qg}^A(x, x_L) = \int_0^1 dz \frac{1}{1-z} [2T_{qg}^A(x, x_L)|_{z=1} - (1+z^2)T_{qg}^A(x, x_L)] \quad (9)$$

comes from the virtual correction to the induced gluon bremsstrahlung process.

If we define the quark energy loss as the energy carried by the radiative gluon in the multiple scattering processes, the total energy loss for a propagating quark in a deeply inelastic scattering (DIS) off a large nucleus is

$$\frac{\Delta E}{E} = \frac{C_A \alpha_s^2}{N_c} \int_0^Q \frac{d\ell_T^2}{\ell_T^4} \int_0^1 dz (1+z)^2 \frac{T_{qg}^A(x, x_L)}{f_q^A(x)}. \quad (10)$$

One can extend the results for medium modified parton fragmentation functions in DIS to the case of quark propagation in a hot medium (either QGP or hot hadronic matter) after it is produced through initial hard processes before the formation of the QGP [15, 22] in high-energy heavy-ion collisions. In this case, we can assume the quark is produced through a hard process such as the virtual-photon-nucleus collisions in Fig. 2 and will interact with partons in the hot medium which is independent

of the initial quark production process. Therefore, we can replace the nucleus state as a product of the initial nucleus state and a thermal ensemble of quasi-particle states in the hot medium,

$$|A\rangle \rightarrow \int \frac{d^3k}{(2\pi)^3 2k^+} \psi_k(y) e^{ik \cdot y} |k\rangle \otimes |A\rangle, \quad (11)$$

and consider only the final state interaction between the produced quark and the bulk medium as illustrated in Fig. 2. Here $f(k, y) = |\psi_k(y)|^2$ is the local phase-space density of the quasi-particle distribution in the medium. We also neglect multiple particle correlations inside the hot medium which can be included through an effective gluon distribution density [15]. Under these assumptions, the quark-gluon correlation function in the HT approach to multiple scattering will take a factorized form,

$$\frac{T_{qg}^A(x, x_L)}{f_q^A(x)} = \frac{N_c^2 - 1}{4\pi\alpha_s C_R} \frac{1+z}{2} \int dy^- 2 \sin^2 \left[\frac{y^- \ell_T^2}{4Ez(1-z)} \right] \times [\hat{q}_R(E, x_L, y) + c(x, x_L) \hat{q}_R(E, 0, y)] \quad (12)$$

where $c(x, x_L) = f_q^A(x + x_L)/f_q^A(x)$ and \hat{q}_R is the generalized jet transport parameter,

$$\hat{q}_R(E, x_L, y) = \frac{4\pi^2 \alpha_s C_R}{N_c^2 - 1} \int \frac{d^3k}{(2\pi)^3} f(k, y) \times \int \frac{d^2q_T}{(2\pi)^2} \phi_k(x_T + x_L, q_T), \quad (13)$$

which depends on the fractional (+) longitudinal momentum transfer x_L from medium gluons [31]. Here $\phi_k(x, q_T)$ is the transverse momentum dependent gluon distribution function from the quasi-particle in the medium,

$$\phi_k(x, q_T) = \int \frac{d\xi^-}{2\pi k^+} d^2\xi_T e^{ixk^+\xi^- - iq_T \cdot \xi_T} \times \langle k | F_\sigma^+(0) F^{+\sigma}(\xi^-, \xi_T) | k \rangle. \quad (14)$$

The two terms in the square brackets of Eq. (12) correspond to two different processes in the multiple scattering. The first term involves (+) longitudinal momentum transfer x_L between the propagating parton and the medium due to final gluon production. It contains what is normally defined as pure elastic energy loss [32]. The second term that is proportional to the normal (or special) transport parameter $\hat{q}_R(E, y) = \hat{q}_R(E, x_L = 0, y)$ corresponds to pure radiative processes. In this paper, we assume $x \gg x_L, x_T$ and only focus on the contribution of radiative energy loss. Therefore, $c(x, x_L) \approx 1$, $\hat{q}_R(E, x_L, y) \approx \hat{q}_R(E, 0, y) \equiv \hat{q}_R(E, y)$. Given the space-time profile of the jet transport parameter $\hat{q}_R(E, y)$, one should be able to calculate the modified fragmentation function according to Eq. (2). The corresponding quark energy loss in Eq. (10) can be expressed as

$$\frac{\Delta E}{E} = \frac{N_c \alpha_s}{\pi} \int dy^- dz d\ell_\perp^2 \frac{(1+z)^3}{\ell_T^4} \times \hat{q}_R(E, y) \sin^2 \left[\frac{y^- \ell_T^2}{4Ez(1-z)} \right], \quad (15)$$

in terms of the jet transport parameter. The jet transport parameter for a gluon is 9/4 times of a quark and therefore the radiative energy loss of a gluon jet is also 9/4 times larger than that of a quark jet. In our following calculations of the hadron spectra in heavy-ion collisions, we will use the same formalism for both quark and gluon modified fragmentation functions but with jet transport parameters that differ by a factor of 9/4 for quark and gluon jets.

III. SINGLE HADRON SPECTRA WITHIN NLO PQCD PARTON MODEL

In this paper, we employ the NLO pQCD parton model for the initial jet production spectra which has been shown to work well for large p_T hadron production in high energy nucleon-nucleon collisions [33]. In a factorized form, the inclusive particle production cross section in $p + p$ collisions can be calculated as a convolution of parton distribution functions inside the proton, elementary parton-parton scattering cross sections and parton fragmentation functions,

$$\frac{d\sigma_{pp}^h}{dyd^2p_T} = \sum_{abcd} \int dx_a dx_b f_{a/p}(x_a, \mu^2) f_{b/p}(x_b, \mu^2) \times \frac{d\sigma}{d\hat{t}}(ab \rightarrow cd) \frac{D_{h/c}^0(z_c, \mu^2)}{\pi z_c} + \mathcal{O}(\alpha_s^3), \quad (16)$$

where $d\sigma/d\hat{t}(ab \rightarrow cd)$ are elementary parton scattering cross sections at leading order (LO) α_s^2 . The next-to-leading order (NLO) contributions including $2 \rightarrow 3$ tree level contributions and 1-loop virtual corrections to $2 \rightarrow 2$ tree processes. We refer to Ref. [20] for a detailed description. The proton parton distribution functions (PDF) $f_{a/p}(x_a, \mu^2)$ are given by the CTEQ6M parametrization [34] where x_a is the fractional momentum carried by the beam partons. The fragmentation function (FF) $D_{h/c}^0(z_c, \mu^2)$ of parton c into hadron h , with z_c the momentum fraction of a parton jet carried by a produced hadron are given by the updated AKK parametrization [35], which is recently improved with new input from the RHIC data, especially for π^\pm , K^\pm , p/\bar{p} , K_S^0 and $\Lambda/\bar{\Lambda}$ particles.

We use a NLO Monte Carlo based program [20] to calculate the single hadron spectra in our study. In this NLO program, the factorization scale and the renormalization scale are chosen to be the same (denoted as μ) and are all proportional to the transverse momentum of the final hadron p_T . As pointed out in Ref. [21], the calculated single inclusive pion spectra within the NLO pQCD parton model for $p + p$ collisions agree well with the experimental data at the RHIC energy using the scale in the range $\mu = 0.9 \sim 1.5p_T$. We find that the calculated π^0 spectra in $p + p$ collisions with the scale $\mu = 1.2p_T$ can fit RHIC data very well and will use the same scale in $A + A$ collisions in our following calculations.

We further assume that the factorized form for large transverse momentum single hadron spectra in NLO pQCD parton model can be applied to heavy-ion collisions,

$$\frac{1}{N_{\text{bin}}^{AB}(b)} \frac{d\sigma_{AB}^h}{dyd^2p_T} = \sum_{abcd} \int dx_a dx_b f_{a/A}(x_a, \mu^2) f_{b/B}(x_b, \mu^2) \times \frac{d\sigma}{d\hat{t}}(ab \rightarrow cd) \frac{\langle \tilde{D}_c^h(z_h, Q^2, E, b) \rangle}{\pi z_c} + \mathcal{O}(\alpha_s^3), \quad (17)$$

where $N_{\text{bin}}^{AB}(b)$ is the number of binary nucleon-nucleon collisions at a fixed impact b of $A + B$ nuclear collisions, $\langle \tilde{D}_c^h(z_h, Q^2, E, b) \rangle$ is the medium modified parton fragmentation function averaged over the initial production position and jet propagation direction, and $f_{a/A}(x_a, \mu^2)$ is the effective parton distributions per nucleon inside a nucleus. For large transverse momentum hadron production, the effect of nuclear modification of the parton distributions is small. We will neglect such nuclear effect in our study here.

According to the definition of the jet transport parameter in Eq. (13), it should be proportional to the local particle density at $\vec{r}_j = \vec{r} + (\tau - \tau_0)\vec{n}$ in either QGP or hadronic phase of the evolving bulk medium along the path of a propagating jet which is a straight line in the eikonal approximation. Here τ_0 is the formation time of the medium and the direction of jet propagation is defined by its azimuthal angle ϕ in the transverse plane. The quark-gluon correlation in Eq. (12) that enters the modified fragmentation function in Eq. (2) will involve an integration over the duration of the jet propagation and depend on the initial production position \vec{r} and propagation direction \vec{n} . In heavy-ion collisions at a fixed impact parameter \vec{b} , the initial jet production cross section is proportional to the overlap function of two colliding nuclei $\int d^2r t_A(r) t_B(|\vec{b} - \vec{r}|)$. One therefore has to average over the initial jet production position and propagation direction to obtain the effective medium modified parton fragmentation function,

$$\langle \tilde{D}_a^h(z_h, Q^2, E, b) \rangle = \frac{1}{\int d^2r t_A(|\vec{r}|) t_B(|\vec{b} - \vec{r}|)} \times \int \frac{d\phi}{2\pi} d^2r t_A(|\vec{r}|) t_B(|\vec{b} - \vec{r}|) \tilde{D}_a^h(z_h, Q^2, E, r, \phi, b). \quad (18)$$

With a given space-time profile of the jet transport parameter, one can therefore use the above effective medium modified fragmentation functions to calculate the large transverse momentum hadron spectra and the the suppression factor (or nuclear modification factor),

$$R_{AB}(b) = \frac{d\sigma_{AB}^h/dyd^2p_T}{N_{\text{bin}}^{AB}(b) d\sigma_{pp}^h/dyd^2p_T}, \quad (19)$$

for characterization of the effect of jet quenching on hadron spectra in heavy-ion collisions [36]. Phenomenological study of the experimental data on the above hadron suppression factor will in turn provide us constraints on the space-time profile of the jet transport parameter $\hat{q}_R(E, y)$.

The computation of the effective medium-modified jet fragmentation function in Eq. (18) involves a 6-dimensional integration which is in addition to the Monte Carlo integration in the NLO pQCD calculation of the single hadron spectra [20]. Numerically, we will compute and tabulate the medium modified fragmentation functions as functions of the initial jet energy E , fractional momentum z and the factorization scale Q^2 for fixed value of impact parameter b . We will then use numerical interpolation of the table for the medium modified fragmentation functions in the NLO pQCD calculation of the single hadron spectra.

IV. BULK MATTER EVOLUTION

Recent phenomenological studies [15, 22–25] have focused on the initial values of the jet transport parameters as constrained by the experimental data. We study in this paper the uncertainty of the extracted initial jet transport parameter due to different models of the dynamical evolution of the bulk medium and in particular the effect of transverse expansion, flow effect, non-equilibrium and phase transition by considering three different models for the bulk evolution. Assuming fast thermalization of the partonic matter in the initial stage of high-energy heavy-ion collisions, we will consider first (1+1)d Bjorken [37] and (1+3)d [38, 39] ideal hydrodynamic evolution of the bulk matter for the calculation of medium modified parton fragmentation functions. Inclusion of shear and bulk viscosity in the viscous hydrodynamics can affect significantly the elliptic flow or azimuthal asymmetry of the final hadron spectra at freeze-out. Their effect on the space-time profile of the bulk medium such as entropy density, however, is much smaller (on the order of a few percent) [40–43] which we will neglect here in the hydrodynamic evolution of the bulk matter for the study of jet quenching. To consider non-equilibrium evolution of the bulk matter and its effect on jet quenching, we will also calculate medium modified hadron spectra with the space-time profile of parton density as given by a parton cascade model [44, 45].

A. (1+1)d Bjorken Expansion

In a (1+1)d Bjorken model [37] for the bulk evolution, the system is assumed to undergo a longitudinally boost-invariant expansion with the (1+1)d ideal hydrodynamic equation,

$$\frac{d\epsilon}{d\tau} = -\frac{\epsilon + P}{\tau}, \quad (20)$$

where ϵ is the energy density, P is the pressure and $\tau = \sqrt{t^2 - z^2}$ is invariant time. For a massless ideal gas equation of state (EOS), the solution of the above ideal hydrodynamic equation leads to a time evolution of the entropy density,

$$s = s_0 \frac{\tau_0}{\tau}, \quad (21)$$

with s_0 the entropy density at the initial time τ_0 . Since the jet transport parameter \hat{q}_R is directly proportional to gluon distribution density and therefore proportional to the particle number or entropy density, we assume that it will have a similar time dependence due to longitudinal expansion. In the (1+1)d Bjorken model, we further neglects the transverse expansion and phase transition. Therefore the transverse profile of jet transport parameter will be given by the initial transverse profile of the parton density which we assume to be proportional to the transverse density of participant nucleons according to the wounded nucleon model of nucleus-nucleus collision [46],

$$\hat{q} = \hat{q}_0 \frac{n_{\text{part}}(\vec{b}, \vec{r})}{n_{\text{part}}(\vec{0}, 0)} \frac{\tau_0}{\tau}, \quad (22)$$

where $n_{\text{part}}(\vec{b}, \vec{r})$ is the transverse density of participant nucleons in nucleus-nucleus collisions with impact parameter b ,

$$n_{\text{part}}(\vec{b}, \vec{r}) = t_A(|\vec{r}|) \left(1 - e^{-\sigma_{NN} t_A(|\vec{b} - \vec{r}|)}\right) + t_A(|\vec{b} - \vec{r}|) \left(1 - e^{-\sigma_{NN} t_A(|\vec{r}|)}\right), \quad (23)$$

and σ_{NN} is the nucleon-nucleon total inelastic cross section, which is set to be $\sigma_{NN} = 42$ mb at the RHIC energy. Here $t_A(\vec{r})$ is the nuclear thickness function,

$$t_A(\vec{r}) = \int_{-\infty}^{\infty} dz \rho_A(\vec{r}, z), \quad (24)$$

and $\rho_A(\vec{r}, z)$ is the single nucleon density in the nucleus normalized to $\int d^2r t_A(\vec{r}) = A$. The total number of participant nucleons in nucleus-nucleus collisions at impact-parameter b is then $N_{\text{part}}(b) = \int d^2r n_{\text{part}}(\vec{b}, \vec{r})$. In the space-time profile of the jet transport parameter in Eq. (22), \hat{q}_0 is defined as the jet transport parameter at the center of the bulk medium in the most central nucleus-nucleus collisions ($b = 0$).

We will consider two different nuclear distributions for $\rho_A(\vec{r}, z)$ in the (1+1)d Bjorken model. One is the Woods-Saxon distribution:

$$\rho_A(\vec{r}, z) = \frac{n_0}{1 + e^{\frac{\sqrt{|\vec{r}|^2 + z^2} - R_A}{a}}}, \quad (25)$$

where $d = 0.662$ fm, $R_A = 1.26A^{1/3}$ fm, and n_0 is the normalization factor given by $\int d^2r dz \rho_A(\vec{r}, z) = A$ [47]. We also consider the simple hard-sphere distribution,

$$\rho_A(\vec{r}, z) = \frac{3A}{4\pi R_A^3} \theta(R_A - \sqrt{|\vec{r}|^2 + z^2}), \quad (26)$$

with $R_A = 1.12A^{1/3}$ for comparison.

In the present work we focus on jet quenching in the 10% most central collisions. By comparing the averaged number of participating nucleons,

$$\langle N_{\text{part}} \rangle = \frac{\int db b N_{\text{part}}(b)}{\int db b}, \quad (27)$$

which is given by experiments for the most 10% central collisions [48], we determine the averaged value of impact-parameter $b = 3.15$ fm for Woods-Saxon nuclear distribution and $b = 2.2$ fm for the hard-sphere distribution.

B. (1+3)d Ideal Hydrodynamical Expansion

To take into account of both longitudinal and transverse expansion in the ideal hydrodynamic description of the bulk matter evolution, we use the output of calculations by Hirano *et al.* [38, 39] for Au+Au collision at the RHIC energy with Glauber collisions geometry and the average impact parameter $b = 3.2$ fm, corresponding to 10% most central events. The initial condition for the (1+3)d ideal hydrodynamic equations is fixed such that the final bulk hadron spectra from the RHIC experiments are reproduced [38, 39]. We use the code provided by Hirano [49] that interpolates the numerical data from the hydrodynamic solution on a space-time grid for energy density, temperature, flow velocity and fraction of QGP phase.

For our purpose, we have to infer parton and hadron number density from the energy density or temperature provided by the hydrodynamic solution, which uses a Bag model for the equation of state (EOS) [50]. In this Bag model, the parton number and energy density in the QGP phase are,

$$\rho^{QGP} = \left(16 \frac{\zeta(3)}{\pi^2} + 36 \frac{3\zeta(3)}{4\pi^2} \right) T^3 \equiv a_1 T^3, \quad (28)$$

$$\epsilon^{QGP} = \left(16 \frac{\pi^2}{30} + 36 \frac{7\pi^2}{240} \right) T^4 + B \equiv b_1 T^4 + B, \quad (29)$$

for three quark flavors. The Bag constant $B = (247 \text{ MeV})^4$ gives rise to a first-order phase transition from the QGP to a hadron resonance gas at the critical temperature $T_c = 170$ MeV.

In our calculation of medium modified parton fragmentation functions we consider jet-medium interaction in both partonic and hadronic phase throughout the evolution of the bulk matter. Neglecting hadron correlation in the medium, the jet transport parameter will be proportional to hadron density and the soft gluon distribution within each hadron. There have been several phenomenological studies [51–53] of jet quenching in deeply inelastic scattering off large cold nucleus as measured by the HERMES [54] experiment. Within the same high-twist approach, the jet transport parameter is found [27] to be

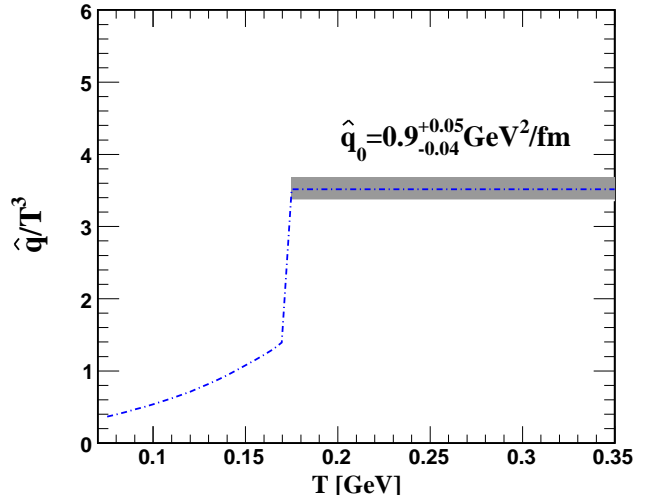


FIG. 3: The temperature dependence of \hat{q}/T^3 .

$\hat{q}_N \approx 0.02$ GeV²/fm at the center of the cold nucleonic matter in a large nucleus. In the (1+3)d ideal hydrodynamic model, the hadronic phase of the medium evolution is considered as a hadron resonance gas, in which the jet transport parameter can be approximate as,

$$\hat{q}_h = \frac{\hat{q}_N}{\rho_N} \left[\frac{2}{3} \sum_M \rho_M(T) + \sum_B \rho_B(T) \right] \quad (30)$$

where $\rho_N = n_0 \approx 0.17$ fm⁻³ is the nucleon density in the center of a large nucleus and the factor 2/3 accounts for the ratio of constituent quark numbers in mesons and baryons. The hadron density at a given temperature T and zero chemical potential is

$$\sum_h \rho_h(T) = \frac{T^3}{2\pi^2} \sum_h \left(\frac{m_h}{T} \right)^2 \sum_{n=1}^{\infty} \frac{\eta_h^{n+1}}{n} K_2 \left(n \frac{m_h}{T} \right), \quad (31)$$

where $\eta_h = \pm$ for meson (M)/baryon (B). In the paper, we will include all hadron resonances with mass below 1 GeV. Other hadron resonance gas models normally include hadrons with mass up to 2 GeV which will only make some differences to our assumed \hat{q}_h close to the phase transition temperature.

With the above approximation for hadron density and jet transport parameter in the hadron phase of bulk medium evolution, the jet transport parameter throughout the evolution of the medium can be expressed as,

$$\hat{q}(\tau, r) = \hat{q}_0 \frac{\rho^{QGP}(\tau, r)}{\rho^{QGP}(\tau_0, 0)} (1 - f) + \hat{q}_h(\tau, r) f, \quad (32)$$

where $f(\tau, r)$ is the fraction of the hadronic phase at any given time and local position and \hat{q}_0 denotes the jet transport parameter at the center of the bulk medium in the QGP phase at the initial time τ_0 . To illustrate the behavior of the jet transport parameter in dense medium,

we plot \hat{q}/T^3 in Fig. 3 as a function of the temperature T according to the above assumptions, where we have used the initial value of $\hat{q}_0 = 0.9_{-0.04}^{+0.05}$ GeV²/fm, as extracted by phenomenological study of experimental data later in this paper, at an initial temperature $T_0 = 369$ MeV in the most central $Au + Au$ collisions at RHIC. Apparently, we have neglected any additional temperature dependence beyond that in Eq. (32). Perturbative calculations [15, 55] in finite temperature QCD with resummed hard-thermal loops give rise to a logarithmic temperature dependence of \hat{q}/T^3 for a fixed value of the strong coupling constant α_s . The same perturbative calculations also lead to somewhat weak jet-energy dependence of the jet transport parameter which we will neglect in this phenomenological study. Therefore, one can consider the exacted jet transport parameter as an averaged value over the range of jet energies in the experimental data.

In order to study the effect of phase transition in the (1+3)d hydrodynamic evolution of the bulk matter in jet quenching, we set $f = 0$ in Eq. (32) and determine the parton density $\rho = a_1[(\epsilon - B)/b_1]^{3/4}$ according to Eq. (28) throughout the bulk evolution, with ϵ given by the (1+3)d hydrodynamic evolution at given space and time. Calculations with this prescription of space-time profile of the jet transport parameter will be labelled as no phase transition in this paper. We can also set $\hat{q}_0^h = 0$ to quantify the hadronic contribution to jet quenching.

The jet transport parameter \hat{q} in Eq. (32) is given in the frame where the medium is at rest. To take into account of the radial flow, one can simply make the following substitute [56, 57]

$$\hat{q} \rightarrow \hat{q} \frac{p^\mu u_\mu}{p_0}, \quad (33)$$

where p^μ is the four momentum of the jet and u^μ is the four flow velocity in the collision frame, which is provided by the solution of the (1+3)d hydrodynamical equations [38, 39]. Such flow dependence effectively decreases (increases) the parton energy loss when the jet propagates along the same (opposite) direction as the flow.

C. (1+3)d Parton Cascade

To study the effect of non-equilibrium evolution of the bulk matter on jet quenching in this paper, we also consider a parton cascade model. The Boltzmann Approach of MultiParton Scatterings (BAMPS) model [44, 45] solves the Boltzmann equation for on-shell gluons with pQCD based interactions, which include elastic scattering, bremsstrahlung and its back reaction. The thermal equilibration process of gluons has been thoroughly investigated within this parton transport model [45, 58]. BAMPS can in principle describe collective flow behavior [59–61] and the nuclear modification factor R_{AA} of jet quenching [62] within a common framework.

In this work we use the output from BAMPS [60] model for central $Au + Au$ collisions with $b = 3.4$ fm at the RHIC

energy. Initial gluons or minijets are produced by binary nucleon-nucleon collisions with a Glauber geometry. The Lorentz contracted nuclei have a longitudinal extent of 0.2 fm. Thus, most minijets are produced at $t = 0.1$ fm/c when two nuclei fully overlap. The strong QCD coupling constant is set to be a constant, $\alpha_s = 0.3$. Gluons freeze out when the local energy density goes below a critical value, which is chosen as $\epsilon_c = 0.6$ GeV/fm³. This corresponds to a critical temperature of $T_c = 175$ MeV in a fully equilibrated gluon gas. In the present implementation of BAMPS there are no hadronization and hadron cascade. Gluons propagate freely (free-streaming) after freeze-out. During this stage we regard one gluon as one hadron according to a parton-hadron duality picture. With these setups the final transverse energy and the elliptic flow v_2 from BAMPS calculations agree with the experimental data at RHIC [59].

We use Eqs. (32) and (33) to evaluate the jet transport parameter in the evolving bulk medium as described by the BAMPS model. The local gluon density and flow velocity are obtained by integrating the local gluon phase space distribution given by BAMPS. The hadron fraction f is either 0 before gluon freeze-out or 1 after gluon freeze-out as a simplification for the hadronization process. By setting $f = 0$ all the time, one effectively neglects the effect of phase transition and the difference in the jet transport parameter in QGP and hadronic phase. The hadron density will be estimated from a free-streaming hadron gas according to an assumption of hadron-parton duality.

V. NUMERICAL RESULTS AND COMPARISONS

With the three different models for the bulk matter evolution and the prescriptions for the evaluation of the jet transport parameter in the evolving medium as described in the last section, we can conduct a systematic analysis of the experimental data on suppression of high p_T hadron spectra within the higher-twist approach to the medium modified jet fragmentation functions. Our aim in this work is to study the theoretical uncertainties associated with the dynamical evolution of the bulk medium and effects of jet hadron interaction in the hadronic medium on jet quenching. Since we assume that the jet transport parameter in the hadronic phase can be estimated from the value as determined in the cold nuclear matter in the DIS off nuclear targets [Eq. (30)], our specific problem in this case is to determine the value of the jet transport parameter \hat{q}_0 at the center of the overlapped region in the central $Au + Au$ collisions in the QGP phase at the initial time τ_0 [see Eqs. (22) and (32)].

Shown in Fig. 4(a) are comparisons between the PHENIX experimental data on R_{AA} for the neutral pion spectra in the 10% most central $Au + Au$ collisions [63] at the highest RHIC energy $\sqrt{s} = 200$ GeV/ n and

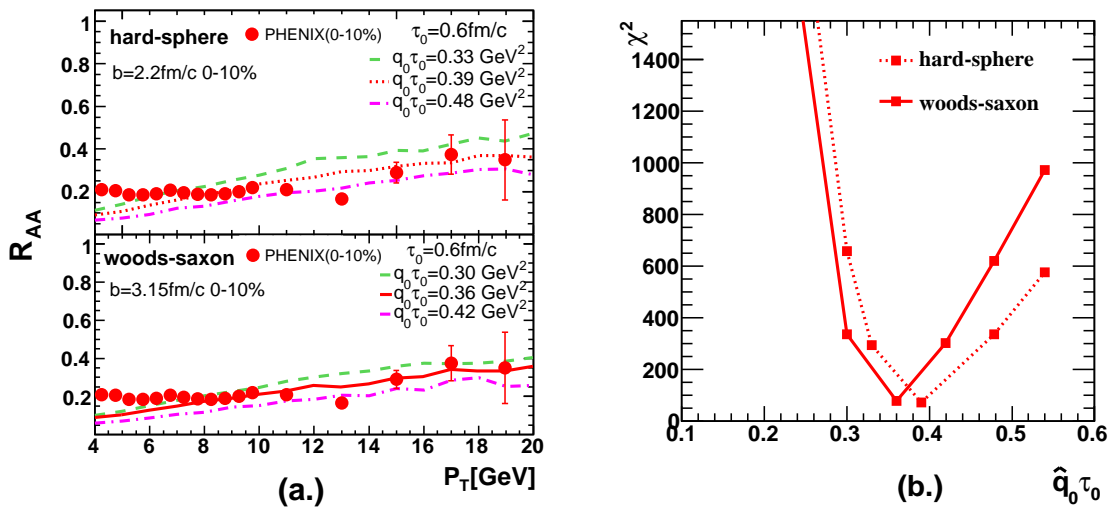


FIG. 4: (color online) (a) Nuclear modification factor at midrapidity for the most 10% central Au+Au collisions at the maximum RHIC energy $\sqrt{s} = 200$ GeV/n. The symbols are the PHENIX data taken from Ref. [63]. The curves are NLO pQCD calculations with three different values of $\hat{q}_0\tau_0$ in the (1+1)d Bjorken model with the Hard-Sphere (upper) and Woods-Saxon (lower) distribution function. (b) The corresponding χ^2 of the fit as a function of $\hat{q}_0\tau_0$.

our NLO pQCD calculations with the medium modified fragmentation functions as given in the higher-twist approach, for three different values of \hat{q}_0 at the initial time $\tau_0 = 0.6$ fm/c, using (1+1)d Bjorken model of ideal hydrodynamical evolution without a phase transition. The upper panel of Fig. 4 (a) shows the results with the hard-sphere nuclear geometry while the lower panel is for Woods-Saxon nuclear distribution. The difference between the calculated suppression factors with hard-sphere and Woods-Saxon nuclear distributions is about 10 percent, due to the small difference in the thickness and overlap functions with these two nuclear distributions.

In the remainder of this paper, we will discuss the determination of initial jet transport parameter and its uncertainties associated with the modeling of the bulk medium evolution. We will carry out systematical χ^2 fits to the experimental data on the suppression factor R_{AA} of neutral pion spectra from the PHENIX experiment [63] with our NLO pQCD calculations that include jet quenching in an evolving bulk medium. We will follow Ref. [64] to carry out a modified χ^2 analysis and obtain the best fit parameters $\hat{q}_0\tau_0$ for each model of bulk medium evolution by minimizing

$$\chi^2 = \sum_{i=1}^N \frac{[y_i + \epsilon_b \sigma_{b_i} + \epsilon_c y_i \sigma_c - y_i^{th}]^2}{\tilde{\sigma}_i^2} + \epsilon_b^2 + \epsilon_c^2, \quad (34)$$

$$\tilde{\sigma}_i = \sigma_i \left(\frac{y_i + \epsilon_b \sigma_{b_i} + \epsilon_c y_i \sigma_c}{y_i} \right), \quad (35)$$

of the fits with respect to two parameters ϵ_b and ϵ_c , where y_i is the central value of experimental data with three

types of uncertainties, σ_i (statistical plus uncorrelated systematics), σ_{b_i} (correlated systematics) and σ_c (normalization uncertainties) for p_T larger than 6.5 GeV/c, and y_i^{th} is the calculated results at each p_T point. Shown in Fig. 4 (b) as two examples are the χ^2 distributions as functions of $\hat{q}_0\tau_0$ ($\tau_0 = 0.6$ fm/c) from the fits with the NLO pQCD calculation with (1+1)d Bjorken model for the bulk medium evolution. The best fit value is $\hat{q}_0\tau_0 = 0.36$ GeV² and 0.39 GeV² for Woods-Saxon and hard-sphere nuclear distribution function, respectively. In the following calculations, we will always use the Woods-Saxon nuclear distribution function.

Listed in Table I are the best fit values of $\hat{q}_0\tau_0$ and the corresponding χ^2 for jet quenching in various models for the bulk medium evolution. We will discuss and compare them in detail in the remainder of this section.

A. (1+1)d Bjorken versus (1+3)d Ideal Hydrodynamical Model

We first compare the results from (1+1)d Bjorken and (1+3)d ideal hydrodynamic model with different options and study the effects of the transverse expansion, radial flow and contributions from jet quenching in the hadronic phase. Comparing the (1+1)d Bjorken and (1+3)d ideal hydrodynamical evolution without radial flow and phase transition it is clear that the transverse expansion cools the system considerably faster in the later stage of the evolution. This faster cooling due to the transverse expansion leads to a faster decrease of the jet transport parameter in the (1+3)d hydrodynamic model than in the (1+1)d Bjorken model as shown in Fig. 5 by the dot-dashed [(1+3)d hydrodynamics] and solid lines [(1+1)d

Model	flow PT	$\hat{q}_0\tau_0(\text{GeV}^2)$	χ^2
(1+1)d Bjorken [W-S]		0.36	78
(1+3)d Hydro		0.42	116
	✓	0.48	80
	✓ ✓	0.54	106
($\hat{q}_0^h = 0$)	✓ ✓	0.78	71
BAMPS		0.72	95
	✓	0.84	84
	✓ ✓	0.96	96
($\hat{q}_0^h = 0$)	✓ ✓	1.17	86

TABLE I: Initial jet transport parameter $\hat{q}_0\tau_0$ and the corresponding χ^2 . The check sign (✓) denotes the inclusion of flow or phase transition (PT) in the calculations, respectively. The initial τ_0 is 0.6 fm/c for hydrodynamic and 0.3 fm/c for BAMPS model.

Bjorken hydrodynamics]. To compensate for this faster cooling, one has to increase the value of the initial jet transport parameter \hat{q}_0 by 17% in the case of (1+3)d hydrodynamic evolution relative to the case of (1+1)d Bjorken expansion in order to fit the measured suppression factor $R_{AA}(p_T)$ for neutral pions in the central $Au + Au$ collisions at RHIC.

Inclusion of the radial flow in the calculation of the jet transport parameter as in Eq. (33) will also change the effective jet quenching throughout the evolution of the bulk medium. Shown in Fig. 6 are the time evolution of the radial flow velocity in (1+3)d hydrodynamics (dashed line). The radial flow velocity in the center of the dense medium (left panel), where jet quenching is the strongest, remains small, at about 0.2, throughout hydrodynamic expansion. In the same figure, we also plot the fraction of the hadron phase (solid lines) as a function of time in the (1+3)d hydrodynamics. The period between $f = 0$ and $f = 1$ indicate the duration of the phase transition or the mixed phase. We notice that at the beginning of the mixed phase the radial flow velocity starts to saturate and even decrease a little. This is mainly due to the mass effect. The energy, approximately $m_T v$, where m_T is the transverse mass, should be the same during the phase transition. Therefore, the radial flow velocity will decrease as particles become massive during the phase transition. Such decrease will be partially compensated by the continued collective expansion which tend to increase the flow velocity. As the phase transition is completed, the radial flow velocity should increase again by further transverse expansion in the hadronic phase and the resonances decays.

The radial flow will reduce the effective jet transport parameter \hat{q} if jets propagate along with it while increase the effective value of \hat{q} if jets propagate against it. After averaging over the direction and initial position of jet production, the effective jet transport parameter is merely reduced by less than 14% [56]. As shown in Table I, this

leads to an increase of \hat{q}_0 about 14% when one includes the effect of radial flow in the (1+3)d hydrodynamic evolution in fitting experimental data on $R_{AA}(p_T)$.

In both (1+1)d Bjorken and two options of the (1+3)d hydrodynamic expansion as discussed above, we have neglected the difference of the jet transport parameters in QGP and hadronic phases. These options are labelled as no phase-transition (PT) by setting $f = 0$ in Eq. (32) and using $\rho^{QGP} = a_1[(\epsilon - B)/b_1]^{3/4}$ in Eq. (28) throughout the evolution even in the mixed and hadronic phase.

In the realistic scenario, jet transport parameter \hat{q}_h in the hadronic phase should be different from that in the QGP phase and we assume that \hat{q}_h is proportional to \hat{q}_N in the cold nuclear medium and the hadron number density as in Eq. (30). With this assumption, there is a discontinuity in \hat{q} as a function of time (or temperature as in Fig. 3) at the end of the mixed phase, as show by the dotted lines in Fig. 5, and the jet transport parameter in the hadronic phase in the later stage of the bulk medium evolution will be smaller than the scenario of no PT in the (1+3)d hydrodynamics. Therefore, one needs a larger value of the initial jet transport parameter \hat{q}_0 , about 13%, to account for the measured suppression factor $R_{AA}(p_T)$ as compared to an evolving bulk medium with the same jet transport parameter throughout difference phases.

To determine the contribution of jet quenching in the hadronic phase, we set $\hat{q}_0^h = 0$ in Eq. (32), assuming parton energy loss only happens in the QGP phase. In this case, the extracted \hat{q}_0 will be about 44% larger (see Table I). This implies that the hadronic phase contributes to about 44% of the total suppression of the high p_T hadron spectra. Such a large contribution is due to the lifetime of the mixed and hadronic phase until the kinetic freeze-out which is longer than the lifetime of the QGP phase, though the hadron density is much smaller than the initial parton density in the QGP phase. A better understanding of the hadronic contribution to the jet quenching is, therefore, important for an accurate extraction of the jet transport parameter in the initial phase of strongly interacting QGP.

B. (1+3)d Parton Cascade versus (1+3)d Ideal Hydrodynamical Model

In a parton cascade model such as BAMPS, the system takes times to reach thermal or partial thermal equilibrium after the initial parton production time, $\tau_0 = 0.3$ fm/c. During this period of parton equilibration, there is entropy production accompanied by rapid expansion. The net effect is a much faster decreasing of the effective temperature [44, 45, 65] and the parton density during the early stage of the bulk medium evolution. The corresponding jet transport parameter in the equilibrating gluonic matter in BAMPS calculation therefore decreases much faster than that in both (1+1)d and (1+3)d ideal hydrodynamic models in the early stage of evolution as shown by the dashed lines in Fig. 5. It is smaller by

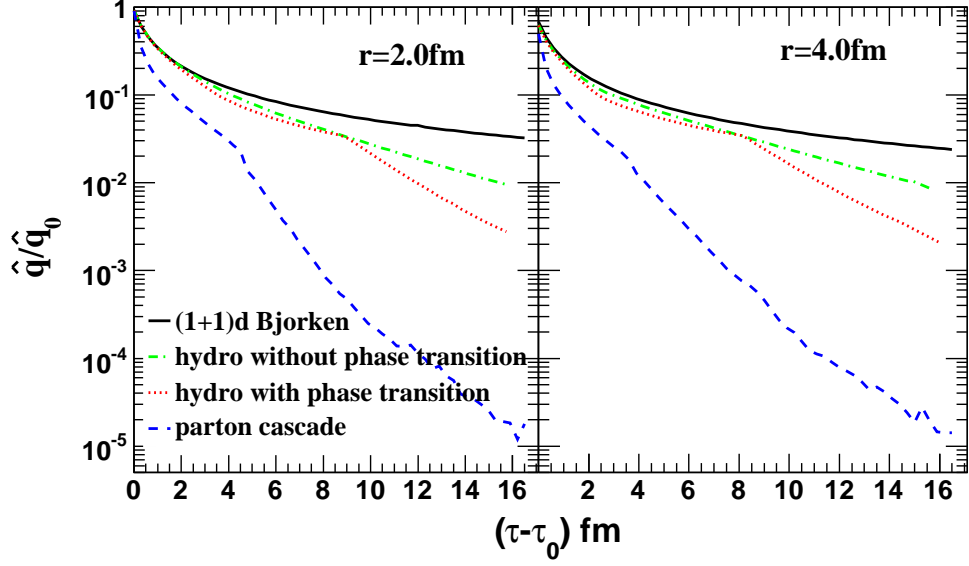


FIG. 5: (color online). Time evolution of the scaled jet transport parameter at position of radius of 2 fm (left panel) and 4 fm (right panel) for various models of the bulk matter evolution. The flow effect in Eq.(33) is not included.

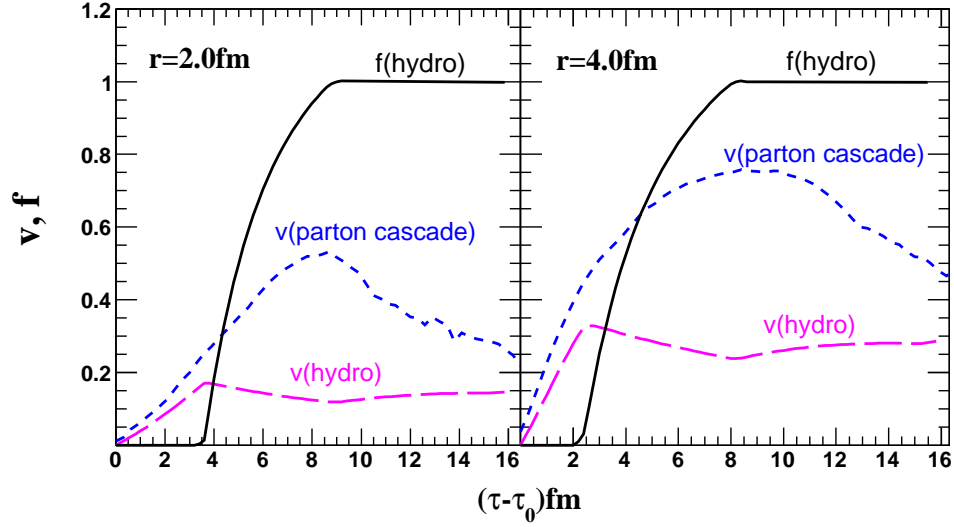


FIG. 6: (color online). The radial flow velocity in the (1+3)d hydrodynamical model and the parton cascade at position of radius of 2 fm (left panel) and 4 fm (right panel). The solid curves show the fraction of the hadron phase in the hydrodynamical model.

more than a factor of 2 before the hadronization. This leads to about 77% increase in the initial value of \hat{q}_0 that is needed to account for the measured suppression of hadron spectra (see Table I). Note that in our calculations jet quenching starts at the thermalization $\tau_0 = 0.6$ fm/c in the ideal hydrodynamic model. However, it starts at $\tau_0 = 0.3$ fm/c in the BAMPS model immediately after the initial gluons are produced and before thermal or partial thermal equilibrium is reached. Such jet medium interaction and parton energy loss during the thermaliza-

tion stage in the BAMPS model will contribute to some additional, though a small fraction, suppression of the final hadron spectra.

In BAMPS, the hadronization of the gluonic matter happens when the local gluon energy density is below $\epsilon_c = 0.6 \text{ GeV} / \text{fm}^3$ and parton-hadron duality is used for the phase-space density of hadrons, which are assumed to freeze out immediately. Such a sudden hadronization and freeze-out scenario implies the change of the hadron fraction f from 0 to 1 at this critical density in the eval-

uation of the jet transport parameter in Eq. (32). The lack of the mixed phase in BAMPS, which lasts for about $5 - 6$ fm/ c in the (1+3)d ideal hydrodynamic evolution as indicated by the duration for the hadron fraction to reach $f = 1$ in Fig. 6, leads to smaller value of the jet transport parameter after the hadronization. Comparing the extracted values of \hat{q}_0 from the phenomenological fit with and without ($\hat{q}_h = 0$) hadronic phase as shown in Table I, the hadronic interaction in BAMPS model contributes to about 22% of the jet quenching effect, which is about a factor 2 smaller than that in the (1+3)d ideal hydrodynamical model.

The large viscous effect in the parton cascade model [59] generally leads to larger radial flow velocity than that generated by an ideal hydrodynamic expansion as shown in Fig. 6. The free-streaming of hadrons immediately after the hadronization also leads to the further increase of the flow velocity. Such larger radial flow velocity in the BAMPS model reduces the effective jet quenching parameter and therefore leads an increase of about 16% in the extracted initial \hat{q}_0 .

The decrease of the radial flow velocity at late times seen in Fig. 6 is a numerical artifact, which comes from the chosen geometry of spatial elements, where particles are collected to calculate the radial flow velocity. Longitudinal length of each spatial element corresponds to a space time rapidity window $|\eta| < 0.25$, while the transverse length is fixed to be 0.3 fm. At late times the longitudinal length is larger than the transverse one, and particles with smaller transverse velocity (larger longitudinal velocity) make up the main part of remaining particles in the spatial elements. This is the reason for the observed decrease of the radial flow velocity. If we choose the longitudinal length being equal as the transverse one at the late times, we would see a continuous increase of the flow velocity due to the free-streaming, before all particles go out of the spatial element. This is, however, a negligible effect on the extraction of \hat{q}_0 , because the hadron density is tiny at late times.

VI. CONCLUSIONS

Using medium-modified fragmentation functions from the high-twist approach to multiple parton scattering we have calculated single inclusive hadron spectra in NLO perturbative QCD parton model. The medium modification to the fragmentation function is very similar in form to the DGLAP correction due to vacuum gluon bremsstrahlung, except that the medium modified splitting function contains information about the properties of the medium through a path-integrated jet transport parameter \hat{q} . Therefore, the medium modified fragmentation function will explicitly depend on the space-time evolution of the bulk medium. We have focused our attention on the dependence of the medium modified fragmentation function on the space-time evolution of the bulk medium and their influence on the suppression of

the single hadron spectra at large p_T .

We specifically considered the effects of transverse expansion, radial flow, jet quenching in hadronic phase and non-equilibrium effect with three different models for the bulk matter evolution in central $Au + Au$ collisions at the RHIC energy: (1+1)d Bjorken hydrodynamic model, (1+3)d ideal hydrodynamical model by Hirano [38, 39] and (1+3)d BAMPS [44, 45] parton cascade model. Since the jet transport parameter is proportional to the particle gluon distribution density of the medium, we have assumed that it will be proportional to the local particle density in both QGP and hadronic phase during the bulk matter evolution. The coefficient of the particle density dependence, which is related to soft gluon distribution per particle, will be different in the QGP and hadronic phase. Assuming a similar density dependence of the jet transport parameter in the hadronic phase as that in a large cold nuclei, but rescaled by the local hadron density and the number of constituent quarks, the only free parameter in the space-time profile is the initial value of the jet transport parameter \hat{q}_0 at initial time τ_0 at the center of the QGP medium in central heavy-ion collisions. We have extracted values of \hat{q}_0 at τ_0 in each model of bulk evolution with different options by fitting the experimental data on the suppression factor $R_{AA}(p_T)$ for high p_T neutral pions and studied the uncertainties in the extracted value of \hat{q}_0 .

By comparing the values of \hat{q}_0 extracted with different options in models for the bulk evolution, we also found that the transverse expansion leads to fast cooling of the hot medium and therefore reduces jet quenching in the later stage of the evolution by about 17%. Radial flow also reduces the effective jet transport parameter by 15%. The phase transition from QGP to hadronic medium further reduces the effective jet transport parameter in the hadronic phase and leads to about 13% reduction of jet quenching effect. Within our model for the form of jet transport parameter due to jet-hadron interaction, the overall contribution to jet quenching from hadronic phase is about 22-44%, depending on the model for evolution of the hadronic phase.

By comparing (1+3)d ideal hydrodynamic and the BAMPS parton cascade model, we found that the non-equilibrium evolution in the early stage of parton cascade leads to faster decrease of the jet transport parameter with time and therefore affects the overall jet quenching the most by 77%, part of which is caused by the lack of mixed phase in the parton cascade model. Such uncertainties can be further reduced by combining parton cascade and hadron cascade with a model of hadronization that can reproduce the EOS during the phase transition as given by lattice QCD calculation.

Acknowledgements

We would like to thank T. Hirano for providing numerical results of (1+3)d ideal hydrodynamic evolution

of the bulk matter in heavy-ion collisions at RHIC and discussions. This work is supported by the NSFC of China under Projects No. 10825523, No. 10635020, by MOE of China under Projects No. IRT0624, by MOST of China under Project No. 2008CB317106 and by MOE and SAFEA of China under Project No. PITDU-B08033, and by the Director, Office of Energy Research, Office of High Energy and Nuclear Physics, Divisions of Nuclear Physics, of the U.S. Department of Energy under Contract No. DE-AC02-05CH11231. The numerical calculations were performed at the Center for Scientific Computing of Goethe University. This

work was financially supported by the Helmholtz International Center for FAIR within the framework of the LOEWE program (Landes-Offensive zur Entwicklung Wissenschaftlich-ökonomischer Exzellenz) launched by the State of Hesse, Germany. X.-N. Wang thanks the hospitality of the Institut für Theoretische Physik, Johann Wolfgang Goethe-Universität and support by the ExtreMe Matter Institute EMMI in the framework of the Helmholtz Alliance Program of the Helmholtz Association (HA216/EMMI) during the completion of this work.

-
- [1] I. Arsene *et al.* [BRAHMS Collaboration], Nucl. Phys. A **757**, 1 (2005) [arXiv:nucl-ex/0410020].
- [2] B. B. Back *et al.*, Nucl. Phys. A **757**, 28 (2005) [arXiv:nucl-ex/0410022].
- [3] J. Adams *et al.* [STAR Collaboration], Nucl. Phys. A **757**, 102 (2005) [arXiv:nucl-ex/0501009].
- [4] K. Adcox *et al.* [PHENIX Collaboration], Nucl. Phys. A **757**, 184 (2005) [arXiv:nucl-ex/0410003].
- [5] J. Adams *et al.* [STAR Collaboration], Phys. Rev. Lett. **91**, 072304 (2003) [arXiv:nucl-ex/0306024]; Phys. Rev. Lett. **91**, 172302 (2003) [arXiv:nucl-ex/0305015].
- [6] S. S. Adler *et al.* [PHENIX Collaboration], Phys. Rev. Lett. **91**, 072301 (2003) [arXiv:nucl-ex/0304022].
- [7] C. Adler *et al.* [STAR Collaboration], Phys. Rev. Lett. **90**, 082302 (2003) [arXiv:nucl-ex/0210033].
- [8] X. N. Wang and M. Gyulassy, Phys. Rev. Lett. **68**, 1480 (1992).
- [9] M. Pluemer, M. Gyulassy and X. N. Wang, Nucl. Phys. A **590**, 511C (1995).
- [10] X. N. Wang, Phys. Rev. C **61**, 064910 (2000) [arXiv:nucl-th/9812021].
- [11] X. N. Wang, Phys. Rev. C **63**, 054902 (2001) [arXiv:nucl-th/0009019].
- [12] M. Gyulassy, I. Vitev and X. N. Wang, Phys. Rev. Lett. **86**, 2537 (2001) [arXiv:nucl-th/0012092].
- [13] X. N. Wang, Phys. Lett. B **579**, 299 (2004) [arXiv:nucl-th/0307036].
- [14] R. Baier, Y. L. Dokshitzer, A. H. Mueller, S. Peigne and D. Schiff, Nucl. Phys. B **484**, 265 (1997) [arXiv:hep-ph/9608322].
- [15] J. Casalderrey-Solana and X. N. Wang, Phys. Rev. C **77**, 024902 (2008) [arXiv:0705.1352 [hep-ph]].
- [16] I. Vitev and M. Gyulassy, Phys. Rev. Lett. **89**, 252301 (2002) [arXiv:hep-ph/0209161].
- [17] X. N. Wang, Phys. Lett. B **595**, 165 (2004) [arXiv:nucl-th/0305010].
- [18] K. J. Eskola, H. Honkanen, C. A. Salgado and U. A. Wiedemann, Nucl. Phys. A **747**, 511 (2005) [arXiv:hep-ph/0406319].
- [19] T. Renk, Phys. Rev. C **74**, 024903 (2006) [arXiv:hep-ph/0602045].
- [20] N. Kidonakis and J. F. Owens, Phys. Rev. D **63**, 054019 (2001) [arXiv:hep-ph/0007268]; B. W. Harris and J. F. Owens, Phys. Rev. D **65**, 094032 (2002) [arXiv:hep-ph/0102128].
- [21] H. Zhang, J. F. Owens, E. Wang and X. N. Wang, Phys. Rev. Lett. **98**, 212301 (2007) [arXiv:nucl-th/0701045]; J. Phys. G **34**, S801 (2007) [arXiv:0804.2370 [hep-ph]].
- [22] A. Majumder, C. Nonaka and S. A. Bass, Phys. Rev. C **76**, 041902 (2007) [arXiv:nucl-th/0703019].
- [23] S. A. Bass, C. Gale, A. Majumder, C. Nonaka, G. Y. Qin, T. Renk and J. Ruppert, Phys. Rev. C **79**, 024901 (2009) [arXiv:0808.0908 [nucl-th]].
- [24] S. A. Bass, C. Gale, A. Majumder, C. Nonaka, G. Y. Qin, T. Renk and J. Ruppert, J. Phys. G **35**, 104064 (2008) [arXiv:0805.3271 [nucl-th]].
- [25] G. Y. Qin and A. Majumder, arXiv:0910.3016 [hep-ph].
- [26] N. Armesto, M. Cacciari, T. Hirano, J. L. Nagle and C. A. Salgado, arXiv:0907.0667 [hep-ph].
- [27] W. T. Deng and X. N. Wang, arXiv:0910.3403 [hep-ph].
- [28] X. F. Guo and X. N. Wang, Phys. Rev. Lett. **85**, 3591 (2000) [arXiv:hep-ph/0005044]; X. N. Wang and X. F. Guo, Nucl. Phys. A **696**, 788 (2001) [arXiv:hep-ph/0102230].
- [29] B. W. Zhang and X. N. Wang, Nucl. Phys. A **720**, 429 (2003) [arXiv:hep-ph/0301195].
- [30] Y. L. Dokshitzer, Sov. Phys. JETP **46**, 641 (1977) [Zh. Eksp. Teor. Fiz. **73**, 1216 (1977)]. V. N. Gribov and L. N. Lipatov, Sov. J. Nucl. Phys. **15**, 438 (1972) [Yad. Fiz. **15**, 781 (1972)]. G. Altarelli and G. Parisi, Nucl. Phys. B **126**, 298 (1977).
- [31] A. Majumder, private communication. Note that the definition of the jet transport parameter \hat{q}_R definite here differs from that in Ref. [22] by a factor of π . Therefore, one has to multiply values of \hat{q}_R extracted from experimental data in this study by a factor of π when compared to that in Ref. [22].
- [32] X. N. Wang, Phys. Lett. B **650**, 213 (2007) [arXiv:nucl-th/0604040].
- [33] J. F. Owens, Rev. Mod. Phys. **59**, 465 (1987).
- [34] H. L. Lai *et al.* [CTEQ Collaboration], Eur. Phys. J. C **12**, 375 (2000) [arXiv:hep-ph/9903282].
- [35] S. Albino, B. A. Kniehl and G. Kramer, Nucl. Phys. B **803**, 42 (2008) [arXiv:0803.2768 [hep-ph]].
- [36] E. Wang and X. N. Wang, Phys. Rev. C **64**, 034901 (2001) [arXiv:nucl-th/0104031].
- [37] J. D. Bjorken, Phys. Rev. D **27**, 140 (1983).
- [38] T. Hirano, U. W. Heinz, D. Kharzeev, R. Lacey and Y. Nara, Phys. Lett. B **636**, 299 (2006) [arXiv:nucl-th/0511046].
- [39] T. Hirano, U. W. Heinz, D. Kharzeev, R. Lacey and Y. Nara, Phys. Rev. C **77**, 044909 (2008)

- [arXiv:0710.5795 [nucl-th]].
- [40] D. Teaney, Phys. Rev. C **68**, 034913 (2003) [arXiv:nucl-th/0301099].
- [41] P. Romatschke and U. Romatschke, Phys. Rev. Lett. **99**, 172301 (2007) [arXiv:0706.1522 [nucl-th]].
- [42] H. Song and U. W. Heinz, Phys. Rev. C **77**, 064901 (2008) [arXiv:0712.3715 [nucl-th]].
- [43] K. Dusling and D. Teaney, Phys. Rev. C **77**, 034905 (2008) [arXiv:0710.5932 [nucl-th]].
- [44] Z. Xu and C. Greiner, Phys. Rev. C **71**, 064901 (2005).
- [45] Z. Xu and C. Greiner, Phys. Rev. C **76**, 024911 (2007).
- [46] A. Bialas, M. Bleszynski and W. Czyz, Nucl. Phys. B **111**, 461 (1976).
- [47] N. Schwierz, I. Wiedenhover and A. Volya, arXiv:0709.3525 [nucl-th].
- [48] J. Adams *et al.* [STAR Collaboration], Phys. Rev. C **72**, 014904 (2005).
- [49] T. Hirano, private communication
- [50] C. Nonaka, E. Honda and S. Muroya, Eur. Phys. J. C **17**, 663 (2000) [arXiv:hep-ph/0007187].
- [51] E. Wang and X. N. Wang, Phys. Rev. Lett. **89**, 162301 (2002) [arXiv:hep-ph/0202105].
- [52] A. Majumder, E. Wang and X. N. Wang, Phys. Rev. Lett. **99**, 152301 (2007) [arXiv:nucl-th/0412061].
- [53] A. Majumder, arXiv:0901.4516 [nucl-th].
- [54] A. Airapetian *et al.* [HERMES Collaboration], Nucl. Phys. B **780**, 1 (2007) [arXiv:0704.3270 [hep-ex]].
- [55] X. N. Wang, Phys. Lett. B **485**, 157 (2000) [arXiv:nucl-th/0003033].
- [56] R. Baier, A. H. Mueller and D. Schiff, Phys. Lett. B **649**, 147 (2007) [arXiv:nucl-th/0612068].
- [57] H. Liu, K. Rajagopal and U. A. Wiedemann, Phys. Rev. Lett. **97**, 182301 (2006) [arXiv:hep-ph/0605178].
- [58] A. El, Z. Xu and C. Greiner, Nucl. Phys. A **806**, 287 (2008).
- [59] Z. Xu, C. Greiner and H. Stöcker, Phys. Rev. Lett. **101**, 082302 (2008).
- [60] Z. Xu and C. Greiner, Phys. Rev. C **79**, 014904 (2009).
- [61] I. Bouras *et al.*, Phys. Rev. Lett. **103**, 032301 (2009).
- [62] O. Fochler, Z. Xu and C. Greiner, Phys. Rev. Lett. **102**, 202301 (2009).
- [63] A. Adare *et al.* [PHENIX Collaboration], Phys. Rev. Lett. **101**, 232301 (2008) [arXiv:0801.4020 [nucl-ex]].
- [64] A. Adare *et al.* [PHENIX Collaboration], Phys. Rev. C **77**, 064907 (2008) [arXiv:0801.1665 [nucl-ex]].
- [65] T. S. Biro, E. van Doorn, B. Muller, M. H. Thoma and X. N. Wang, Phys. Rev. C **48**, 1275 (1993) [arXiv:nucl-th/9303004].